

ANALYSIS AND CALIBRATION OF LORAN-C SIGNALS IN THE LOWER St. LAWRENCE AREA USING GPS

by G. LACHAPELLE ¹, B. TOWNSEND ¹, D. HAINS ²

Abstract

Loran-C signals along and in the Lower St. Lawrence River, namely between Québec City and the Gaspesia Peninsula on the south shore, between Québec City and Havre-Saint-Pierre on the North Shore, and between Québec City and Anticosti Island in the river, were analyzed using a mobile Loran-C coverage validation and calibration system consisting of analog and digital Loran-C receivers, differential GPS and data logging systems. The road measurements were made successively during February-March and July-August 1991 to analyse seasonal effects. The signals received from the East Coast Canada Chain (5930M, X, Y, Z) and the Northeast U.S. Chain (9960M, W, X) are discussed herein. The Field Strength and Signal to Noise Ratio measurements are compared with predicted values using various models for conductivity and atmospheric noise. The Time Difference (TD) measurements are first compared between forward and reverse runs along the road profiles to ascertain the quality and reliability of the system utilized. The differences between Winter and Summer TD measurements are then analyzed. A relatively small but significant seasonal effect is found. The GPS-derived TD distortions are compared with those derived using various models for the combined effect of the primary, secondary and additional secondary phase lags. The differences between measured and modeled distortions reaches several μ s. The effect of these differences on Loran-C positions is found to reach several hundred metres in many cases. Conclusions related to the results presented herein are made, together with recommendations pertaining to the use of these results and future investigations.

¹ Department of Geomatics Engineering, The University of Calgary, 2500 University Dr., N.W., Calgary, Alberta, Canada, T2N 1N4.

² Canadian Hydrographic Service (Québec Region), Institut Maurice-Lamontagne, 850 Route de la Mer, Mont-Joli, Québec, G5H 3Z4.

INTRODUCTION

The major objectives of the project reported herein are the analysis and calibration of the Loran-C signals available in the Lower St. Lawrence area of Québec under both Winter and Summer conditions. The area under consideration and the Loran-C transmitters available are shown in Figure 1. The project was undertaken during 1991-1992 in support of the Canadian Hydrographic Service's continuous chart updating programme. Loran-C is a regulatory system for marine navigation in Canadian waters and Loran-C lattices are printed on charts where Loran-C is available. The roads and ship tracks actually observed during Winter and Summer 1991 are shown in Figure 2. The two Loran-C chains which were used are the Northeast U.S. Chain and the Canadian East Coast Chain. Only 7930M and W were received from the Labrador Chain. These signals coincide with 5930Y and Z of the Canadian East Coast Chain and were not considered in the analysis. The power of the transmitters varies between 400 and 1000 kW and the transmitter coordinates are available in the World Geodetic System 1984 [CCG 1990, USNO 1992]. The Horizontal Dilution Of Precision (HDOP) of both chains and a combination thereof is shown in Figure 3.

Loran-C is affected by the following time- and position-dependent effects [e.g., LACHAPPELLE & TOWNSEND, 1990]:

(i) Time-dependent effects:

- Variations of the Primary Factor (PF), i.e., variations of the tropospheric refractivity along the propagation path due to weather fronts and large weather/climate variations between coastal areas and hinterlands, a situation which prevails in the present case, as can be seen from Figure 1. These effects are mostly compensated by the Loran-C area monitors but residual effects may be significant. The magnitude of these effects is a function of many parameters and may reach 100 m on the measured TD's in extreme cases [e.g., SAMADDAR, 1980].
- Signal transmission synchronization: The area monitors are used to maintain synchronization within 30 to 50 ns, i.e., 10 to 17 m, in terms of TDs. This effect is not considered significant in view of other overwhelming effects.
- Time-dependent variations in the conductivity of the ground/ice: In the case of the ground, these variations would not normally be considered significant unless the level of humidity of the ground is subject to large seasonal variations. In the case of sea ice, experiments made in the Beaufort Sea by the Canadian Hydrographic Service in the late 70s and early 80s with Decca and Loran-C did not reveal significant variations [GRAY 1975; EATON et al 1982]. In the case of salt water with a lower salinity level than normal sea water, as in the case of the Lower St. Lawrence, the effect is likely to be minimal, similarly to that of normal sea ice.

- The atmospheric noise caused by nearby and distant thunderstorms and lightning bursts in the 90 - 110 kHz frequency band of the amplitude modulated Loran-C signal. This noise does not affect the propagation speed but affects the detection level of the signals and, therefore, the measuring accuracy of the receiver and the effective range of the transmitters. In the area of interest, predicted diurnal variations reach 20 dB, with the lowest atmospheric noise in the morning and the highest in the evening [CCIR 1988a]. Predicted seasonal variations reach 12 dB, with the lowest level in the Winter. With such large variations and a minimum of about -10 dB required for effective signal detection by most receivers, the effective range of transmitters can in principle vary by several hundred km between nighttime and daytime or between Winter and Summer conditions.

(ii) Time independent/position-dependent effects:

- Some 80% to 90% of the effect of conductivity under normal conditions are time-independent but position-dependent. The effect of mixed terrain-water propagation paths further complicates the situation as the case of the Lower St. Lawrence. Residual position effects can easily exceed a few hundred metres. Signal attenuation may also result, affecting the reliability of Loran-C in local areas.
- The terrain effect can cause position distortions between 500 m and 1,000 m in mountainous areas, as demonstrated by LACHAPPELLE et al. [1992]. In the Lower St. Lawrence, this effect may be significant in local areas in view of the relatively rugged topography between transmitters and users. The effect may reach a few hundred metres in some cases. Signal attenuation may also result in local areas due to diffraction effects.

A horizontal dilution of precision (HDOP) greater than 1 will amplify the above effects. The above position-dependent errors can be reduced by proper calibration using a positioning system which is not affected by the same effects. Calibration results, once verified, need not be repeated, thus avoiding recurring costs. Adequate calibration has the potential of increasing the accuracy of Loran-C to 100 m along the calibration routes, in addition to improving the reliability of Loran-C for marine navigation.

The concept of calibrating Loran-C with GPS is straightforward. Loran-C ground waves are affected by position dependent conductivity and terrain effects while GPS space waves are not. Differential GPS yields an accuracy of 5 m or better, which is more than sufficient for Loran-C TD calibration. Although atmospheric effects can be taken into account to a certain extent, it is not possible to separate completely the position dependent conductivity and terrain effects from the time dependent atmospheric and other effects, the latter effects being of the order of 50 to 100 m. The Loran-C biases obtained through a comparison with GPS will therefore represent the position dependent effects with an accuracy of the order of 100 m. This is a major improvement over "uncalibrated" Loran-C positions which could be in error by several hundred metres.

METHODOLOGY

Equipment

The LORCAL² configuration used during the Winter and Summer 91 field campaigns is shown in Figure 4 and consisted of the following components: (i) an analog Accufix 520 Loran-C receiver to measure the signals on the Northeast U.S. Chain, (ii) a digital LocUS Pathfinder receiver to measure the signals on the Canadian East Coast Chain, (iii) two Ashtech LD-XII units for DGPS operation, and PC-based data logging systems for the GPS monitor and the mobile system. The system was previously tested using a comparison of forward and reverse measurements as described in [LACHAPPELLE et al, 1992]. The error budget of LORCAL² is as follows: (a) internal Loran-C receiver noise, ≤ 50 m, (c) effect of GPS time synchronization error, ≤ 5 m, and (d) differential GPS, 3 - 10 m, HDOP ≤ 5 , drms. The overall accuracy of the system is the quadratic sum of the above errors, namely 52 m or $0.17\mu\text{s}$ (1σ).

Field Measurements

The field measurements was undertaken into two phases, namely: Phase 1 (February-March 91), during which measurements were made along the 1,600 km of land roads shown in Figure 2. Phase 2 (July-August 91), during which measurements were made along the same land routes as above and along the ship routes shown in Figure 2. All GPS observations were made in DGPS mode with the monitor unit located at the Canadian Hydrographic Service - Québec Region (CHS-IML on Figure 2). The following Loran-C measurements were made at intervals of five seconds to provide the continuous profiles required for a thorough analysis of the signals: Signal-to-Noise Ratio (SNR) of the incoming signals, TDs, and Field Strength (FS). GPS code and carrier phase measurements were made at intervals of two seconds to provide sufficiently dense data for the linear interpolation of GPS-derived TDs. All land routes were observed in the forward and reverse directions to provide an adequate quality control of the measurements.

Data Reduction

The differential GPS measurements were reduced using a carrier phase smoothing of the code approach (CANNON & LACHAPPELLE, 1992). Differential range corrections were calculated every 5 or 10 s at the monitor station and applied, in post-mission, to the carrier phase smoothed pseudoranges at the vehicle. Since the GPS and Loran-C measurements were generally made at different epochs on the vehicle, the DGPS positions of the Loran-C measurements were obtained through a linear interpolation. GPS was used under the following conditions: HDOP ≤ 5 , with no height constrained. Height fixing was allowed for a period of up to 5 minutes on the vehicle to improve the GPS HDOP. This was done when the HDOP without height constraint exceeded 5 or when only 3 satellites were available. An average height obtained during the previous 5 to 10 3-D position fixes was used as

constraint. On the ship, the height was always constrained to the GPS height of the antenna. GPS outages (i.e., HDOP > 5) for periods greater than 10 seconds were no longer valid and no Loran-C corrections were calculated. The Loran-C SNR constraints were set as follows: SNR > -10 dB (Accufix 520 receiver), SNR > -20 dB (LocUS Pathfinder receiver), and FS > 30 dB.

The Loran-C TD distortion DTD, is defined herein as

$$DTD = TD_{\text{Loran-C}} - TD_{\text{GPS}}$$

where $TD_{\text{Loran-C}}$ is the measured Time Difference, and TD_{GPS} is the corresponding Time Difference calculated using DGPS positions. All DTDs obtained within 2-km intervals were averaged to obtain a single value for the centre of each interval. This procedure was carried out only if at least five measurements were available in the interval. Otherwise, no value was calculated. The maximum number of measurements in a 2-km section reached 30.

ANALYSIS OF MEASUREMENTS

Field Strength (FS), Atmospheric Noise (N_{atm}) and SNR Analysis

The Field Strength and Atmospheric Noise (N_{atm}) are given $\mu\text{V m}^{-1}$ or in dB referred to $1\mu\text{V m}^{-1}$. Conversion from $\mu\text{V m}^{-1}$ to dB is accomplished by using the following formula:

$$\text{dB} = 20 \log X$$

where X is either FS or N_{atm} in $\mu\text{V m}^{-1}$. The FS, at 100 kHz, is mainly a function of transmitter power and conductivity along the propagation path. If one assumes that the conductivity is known and constant along the propagation path, FS can be precisely calculated using finite formulae [JOHLER et al, 1956, CCIR, 1988b]. These formulae have been used to generate graphs giving FS as a function of distance for a nominal radiated power, e.g. 1 kW [ROHAN, 1991]. FS for any other radiated power P is then given by

$$FS(\mu\text{V m}^{-1})_p = FS(\mu\text{V m}^{-1})_{1 \text{ kW}} \sqrt{P(\text{kW})}$$

or

$$FS(\text{dB})_p = FS(\text{dB})_{1 \text{ kW}} + 20 \log \{\sqrt{P(\text{kW})}\}.$$

FS curves calculated using the above technique are given in Figure 5 for selected ground conductivities as a function of the distance from the source for a radiated power of 400 kW. The difference between the best conductor, i.e., seawater at 5 S m^{-1} (1 Siemen = 1 mho), and a very poor conducting soil at 0.001 S m^{-1} , grows as a function of the distance from the transmitter. At 1,000 km, the difference is nearly 10 dB. When the conductivity varies along the path, FS can be calculated using Millington's method [SAMADDAR, 1979]. Since the exact conductivity along the propagation path is not exactly known, however, especially in the case of overland paths, an average conductivity is used to estimate FS. This was done in the present

case. The a priori value used for the area under consideration was 0.001 S m^{-1} [HAMILTON, 1987].

The atmospheric noise is not measured directly by a Loran-C receiver but derived using the following equation:

$$N_{\text{atm}_{\text{meas}}} = FS_{\text{meas}} - \text{SNR}_{\text{meas}}$$

N_{atm} is a function of thunderstorm activities around the world and has been estimated by CCIR [1988a] for the 1 MHz frequency using data collected at various locations. The estimated values are a function of location, season, and time of day. The CCIR report gives world maps showing estimated noise in dB for each period of 4 hours for each season. The rms noise field strength is given by

$$N_{\text{atm}}(\text{dB}) = F_a - 95.5 + 20 \log f_{\text{MHz}} + 10 \log b$$

where F_a is the rms noise value extracted from the maps (at 1 MHz) and reduced to f_{MHz} , the Loran-C frequency (0.1 MHz) using curves given in the report, and b , the Loran-C bandwidth in Hz, i.e., 20,000 Hz. The above formula was used to calculate N_{atm} for the area under consideration and the results are shown in Table 1. Diurnal variations of up to 15 dB are noted. The differences between Summer and Winter reached 15 dB, the noise being higher in Summer. An average atmospheric noise value of 61 dB for the areas covered by the two Loran-C chains has recently been predicted by the U.S. Department of Transportation [U.S. DoT, 1992]. This constant value is considerably higher than the values given in Table 1 and was obtained by assuming the worst case, which occurs during late evenings in Summer. In order to obtain such a high value from the CCIR maps, one would select the largest N_{atm} corresponding to Summer evenings in the area and add another 10 to 20 dB as a safety factor. Both the constant 61 dB value and the values given in Table 1 were tested. An analysis of both Summer and Winter data showed no significant diurnal or seasonal variations. Moreover, the measured atmospheric noise agreed with the predicted constant value of 61 dB within a few dBs.

As an example, measured and predicted FS , SNR and N_{atm} values obtained in Winter 91 are intercompared at representative points in Table 2. The predicted SNR was calculated as follows:

$$\text{SNR} = FS_{\text{meas}} - N_{\text{atm}_{\text{pred}}}$$

The DSNR 's were obtained using the N_{atm} values of Table 1, while the DSNR_{N_c} 's were obtained using a constant N_{atm} of 61 dB. The differences between measured and predicted FS are generally within a few dBs for overland paths. This indicates that the conductivity of 0.001 S m^{-1} selected to predicted FS values is realistic. For mixed land-water paths, the best agreement, not shown in Table 2, was obtained using Millington's method. The recovery effect was noticeable at many locations. The differences between measured and predicted SNR values are much smaller when a constant value of 61 dB is used. Similar results were obtained for the Winter data.

Forward versus Reverse DTD Road Measurements

A comparison of forward and reverse DTD measurements made along the road profiles provides a reliable estimate of their repeatability and of the performance of the LORCAL² system. Summary statistics are given in Table 3. These comparisons are based on 2-km averages. Outliers due to local signal interference and averaging effects caused by local topography were removed prior to deriving these statistics. The mean differences between the forward and reverse DTDs are $\leq |0.1 \mu\text{s}|$, which is considered satisfactory. The rms differences are below $0.24\mu\text{s}$, which is within the *a priori* accuracy of $0.17\mu\text{s} \sqrt{2}$ estimated for the LORCAL² system (Fig. 4).

Winter versus Summer DTD Measurements

The Winter and Summer road measurements were made primarily to assess seasonal effects on DTDs. This effect was analysed by first averaging the forward and reverse DTD measurements made in Winter and Summer, respectively. The differences between Winter and Summer averages are summarized in Table 4. The mean differences reach $-0.24\mu\text{s}$, which is equivalent to a range difference of 72 m. Seasonal differences are usually due to variations in the primary and secondary phase lags. In order to test whether seasonal variations in the primary phase lag could account for the above differences, the PF effect on the TD measurements made on the Canadian East Coast Chain was calculated using two values for refractivity, namely 310 and 330. These values correspond to extreme Winter and Summer conditions, respectively, in the area of the survey [SEGAL & BARRINGTON, 1977]. The average difference between the two sets of TDs generated with the above refractivity coefficients was $0.04\mu\text{s}$, well below the average value of $0.20\mu\text{s}$ derived from Table 4. The seasonal variations measured here are possibly caused by changes in conductivity between Winter and Summer. Nevertheless, these variations are not sufficiently large to use seasonally adjusted Loran-C grid corrections for marine navigation in the area.

Across-Chain (5930 Versus 9960) TD Comparison

The 5930X TD is given by

$$\text{TD}(5930\text{X}) = \text{T}(5930\text{M-Caribou}) - [\text{T}(5930\text{x-Nantucket}) - 13131.88\mu\text{s}]$$

where $13131.88\mu\text{s}$ is the fixed emission delay of 5930X [CCG, 1990; USNO, 1992]. The 9960X and 9960W TDs are given by

$$\text{TD}(9960\text{X}) = \text{T}(9960\text{M-Seneca}) - [\text{T}(9960\text{X-Nantucket}) - 26969.93\mu\text{s}]$$

$$\text{TD}(9960\text{W}) = \text{T}(9960\text{M-Seneca}) - [\text{T}(9960\text{W-Caribou}) - 13797.20\mu\text{s}]$$

If all transmitters in both chains were transmitting on precisely the same time scale, we would expect the following relationship to hold, within the accuracy of the measurements:

$$[TD(9960X) - TD(9960W)] - TD(5930X) = 0$$

The above differences are shown in Figure 6 for representative road and ship measurements. The road measurements taken in forward and reverse directions both during Winter and Summer 91 were averaged. The ship measurements were taken during Summer 91. An average difference of 0.46 to 0.48 μ s is present. The standard deviation of one difference varies between 0.07 and 0.11 μ s. The average difference of nearly 0.5 μ s, which corresponds to a range difference of some 150 m, is due to time scale variations between the transmitters, such as biases in the emission delays. For instance, the area monitors control the TDs in their respective areas to ensure a high degree of position repeatability. The area monitors for 5930X, 9960X and 9960W are located in Montague, Prince Edward Island, Sandy Hook, New Jersey, and Cape Elizabeth, Maine, respectively. Initial differential position errors between the monitors and the transmitters, for instance, could cause the above constant difference of 0.5 μ s. A similar effect between the two chains has been observed in the northeast United States [PETERSON, 1992].

Modelled Versus GPS-Derived DTDs

In order to analyse the differences between modelled and GPS-derived DTDs, a series of numerical tests was conducted. The primary phase lag (PF) was modelled using a constant refractivity of 320 which corresponds to a refractive index of 1.000320. The combined effect of the secondary (SF) and additional secondary (ASF) phase lags was modelled using successive values of 5, 0.005 and 0.001 S m⁻¹ for conductivity. The secondary phase lag is the phase delay due to propagation over sea water. The additional secondary phase lag is the additional phase delay due to propagation over land. The highest value (5 S m⁻¹) corresponds to a propagation path over sea water (ASF = 0). The lowest value corresponds to the estimated soil conductivity in the area covered by the two chains [HAMILTON, 1987]. The combined effect of the secondary and additional secondary phase lags as a function of the distance from the transmitter is shown in Figure 7 for selected conductivities [FRANK, 1983].

The results are summarized in Tables 5 and 6 for the road and ship profiles, respectively. The mean residual DTDs when no phase factor is applied reaches -4.6 μ s. The application of PF, SF and ASF corrections with a conductivity of 5 S m⁻¹ results in the best agreement, both in terms of lower mean and rms values, in the case of the Canadian East Coast Chain. This is due to the effect of sea water on most propagation paths from the 5930 transmitters, as can be seen from Figure 1. The use of a conductivity value of 0.001 S m⁻¹, however, results in the best agreement in the case of the Northeast U.S. Chain. The use of Millington-Plessey's technique [SAMADDAR, 1979] to model the effect of SF and ASF along the mixed paths would likely improve the agreement between GPS-derived and modelled DTDs significantly.

The residual DTDs constitute the accuracy gain obtained by using GPS to calibrate the Loran-C TDs. The mean and rms values of these residuals exceed 1 μ s, i.e., 300 m, in many cases. The effect of these residuals on Loran-C positions is a function of the transmitter geometry. Resulting latitude and longitude errors are shown in Figures 8 to 11 for the following TD combinations.

- Canadian East Coast Chain: 5930X, Y and Z (North and South shore Roads Profiles)
- Northeast U.S. Chain: 9960W and X (North and South shore Roads Profiles)
- Combined Chains/ 5930X, 5930Y, 9960W and 9960X (Ship Profiles).

Since a conductivity of 5 S m^{-1} was used, the position distortions represent the ASF effect. For each case, the mean, root mean square and standard deviation are given. The maximum distortion reaches -1,500 m in latitude in the case of the combined chain solution. The rms values vary from 200 to 900 m. The large effects show that uncalibrated Loran-C would not deliver the prescribed accuracy of 460 m (0.25 nm). The lowest standard deviations are obtained when using the combined chains. This is not surprising since the ASF effect is averaged out more effectively in this case through the availability of four TDs. The real advantage of multi-chain measurements however is the gain in reliability, in addition to a slightly better geometry, as shown in Figure 3.

A comparison of the TD distortions reported herein with values determined previously by the Canadian Hydrographic Service at selected points for chart lattice construction revealed a satisfactory agreement [GRAY, 1992].

CONCLUSIONS AND RECOMMENDATIONS

The major conclusions of this Loran-C calibration and analysis are as follows: The performance of the LORCAL² system were satisfactory and the objectives of the study were met. The measured Loran-C FS and SNR agreed best with predicted values when a ground conductivity of 0.001 S m^{-1} and an atmospheric noise of 61 dB were used. The GPS-derived Loran-C distortions measured both on the Canadian East Coast and Northeast U.S. Chain in the survey area reach nearly $5\mu\text{s}$. The residual distortions still present once the primary, secondary and additional secondary factors (using a uniform propagation path assumption) are removed, are minimized when using a conductivity value of 5 S m^{-1} on the East Coast Canada Chain and 0.001 S m^{-1} on the Northeast U.S. Chain. The effect of these residual distortions on Loran-C derived positions reaches several hundred metres and is a function of the transmitter geometry.

Two recommendations arise from the results presented herein. The use of Millington's and Millington-Plessey's techniques to predict FS and SF+ASF, respectively, over mixed propagation paths, may result in a better agreement between predicted and measured field strengths in some areas, and in a better modelling of the Loran-C distortions measured by GPS than the use of the uniform propagation path models tested herein. Future Loran-C field analyses should be made with low noise multi-chain digital receivers to improve performance. Field experiments with the enhanced LORCAL² system made in 1992, and based on the use of multi-chain Jet 7201 receivers, have resulted in more consistent and generally better results than those obtained with the earlier system used herein [LACHAPELLE & TOWNSEND, 1993].

References

- CANNON, M.E. and G. LACHAPPELLE (1992): Analysis of a High Performance C/A Code GPS Receiver in Kinematic Mode. *Navigation*, Vol. 39, No. 3, The Institute of Navigation, Alexandria, VA, USA, pp. 285-299.
- CCG [1990] Radio Aids to Marine Navigation (Atlantic and Great Lakes). Publication TP146E, Telecommunications and Electronics Directorate, Canadian Coast Guard, Transport Canada, Ottawa, Canada.
- CCIR [1988a] Characteristics and Applications of Atmospheric Radio Noise Data. CCIR Report No. 322-3, International Telecommunications Union, Geneva, Switzerland.
- CCIR [1988b] World Atlas of Ground Conductivities. CCIR Report No. 717-2, International Telecommunications Union, Geneva.
- EATON, R.M., M. MCALONEY, A. MORTIMER, E. SCHENING and B. WALDOCK [1982] Beaufort Sea Loran-C Tests. *Canadian Journal of Aeronautics*, Vol. 28, No. 1, pp. 9-18.
- FRANK, R.L. (1983) Current Developments in Loran-C. *Proceedings of the IEEE*, Vol. 71, No. 10, pp. 1127-1139.
- GRAY, D.H. [1975] Propagation Velocity of Decca Frequency Transmissions Over Sea Ice. *The Canadian Surveyor*, Vol. 29, No. 3, pp. 277-288.
- GRAY, D.H. [1992] Personal Communication. Canadian Hydrographic Service. November.
- HAMILTON, G. [1987] Extension of Canadian Loran-C Coverage. IRRD No. 291115, Roads and Transportation Association of Canada, Ottawa, Canada.
- JOHLER, J.R., W.J. KELLAR, and L.C. WALTERS [1956] Phase of the Low Radiofrequency Groundwave. Circular 573, National Bureau of Standards, U.S. Department of Commerce.
- LACHAPPELLE, G., and B. TOWNSEND [1990] En Route Coverage Validation and Calibration of Loran-C with GPS. *Proceedings of GPS'90*, Institute of Navigation, Washington, D.C., pp. 199-205.
- LACHAPPELLE, G., and B. TOWNSEND (1993) GPS/Loran-C: An Effective System Mix for Vehicular Navigation in Mountainous Areas. *Navigation*, Vol. 40, No. 1, The Institute of Navigation, Alexandria, VA, USA (in press).
- LACHAPPELLE G., B. TOWNSEND and B.B. MYERS [1992] Analysis of Loran-C Performance in the Pemberton Area, B.C. *Canadian Journal of Aeronautics*, Canadian Aeronautics and Space Institute, Ottawa, Canada, Vol. 38, No. 2, pp. 52-61.
- PETERSON, B. [1992] Personal Communication, U.S. Coast Guard Academy, New London, Connecticut, October.
- ROHAN, P. [1991] Introduction to Electromagnetic Wave Propagation. Artech House, Boston, USA.
- SAMADDAR, S.N. [1979] The theory of Loran-C Groundwave Propagation - A Review. *Navigation, Journal of the Institute of Navigation*, Washington, D.C., USA, Vol. 26, No. 3, pp. 173-187.
- SAMADDAR, S.N. [1980] Weather Effect on Loran-C Propagation. *Navigation, Journal of The Institute of Navigation*, Vol. 27, No. 1, pp. 39-53, Washington, D.C., USA.
- SEGAL, B., and R.E. BARRINGTON [1977] The Radio Climatology of Canada - Tropospheric Refractivity Atlas for Canada. CRC Report No. 1315-E, Department of Communications, Ottawa, Canada.
- US DOT [1992] FAA LORAN Coverage Diagrams. Prepared by National Field Office for LORAN Data Services, DTS-502, Volpe National Transportation Systems Center, Cambridge, Massachusetts, USA.
- USNO [1992] Time Service Announcement, Series 9-Stations, No. 319, 27 January, U.S. Naval Observatory, Washington, D.C., USA.

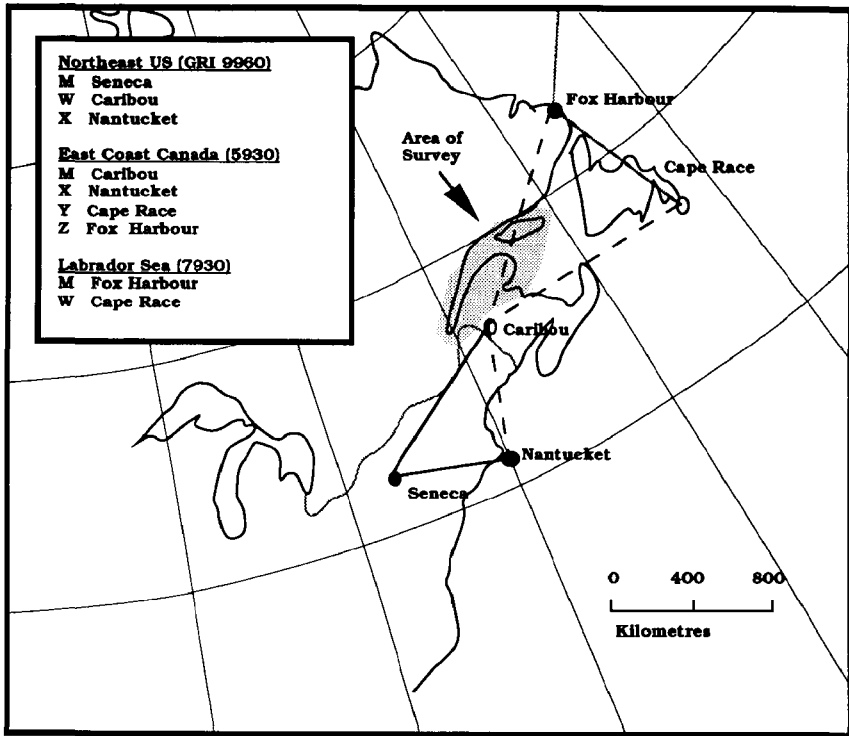


FIG. 1.- Survey Area and Loran-C Transmitters Available.

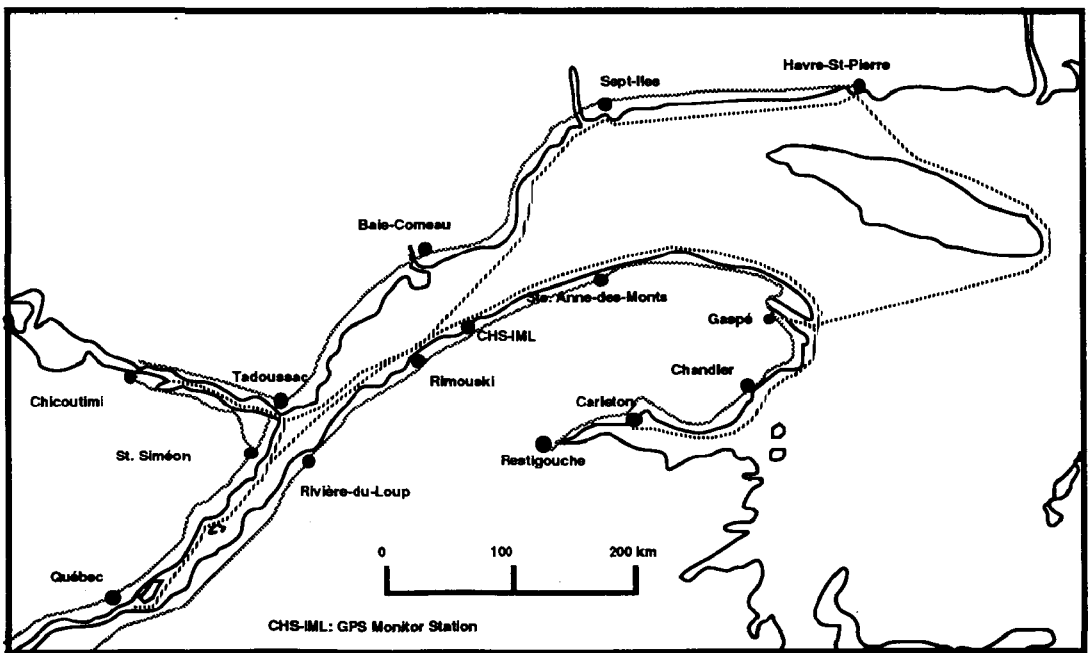
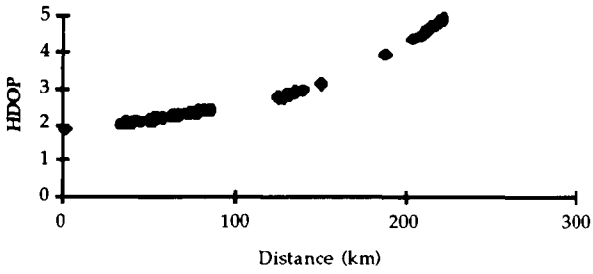
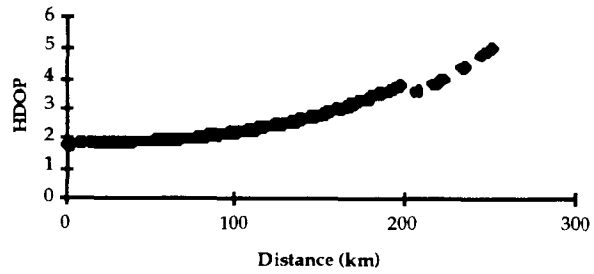


FIG. 2.- Land Roads and Ship Tracks Observed - Winter and Summer 1991.

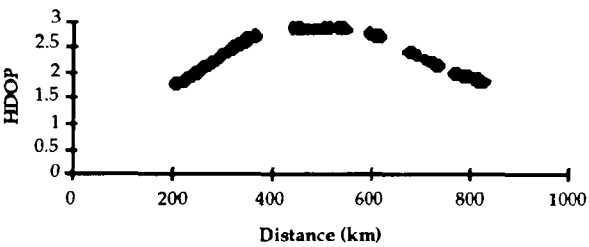
Québec to Tadoussac, TDs = 9960W 9960X



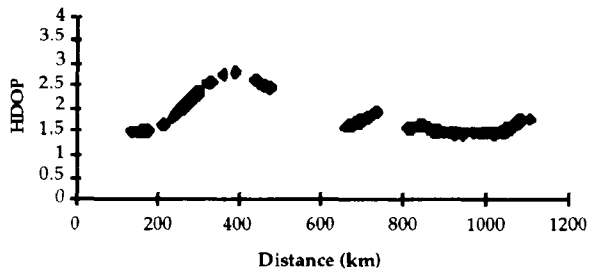
Québec to Rimouski, TDs = 9960WX



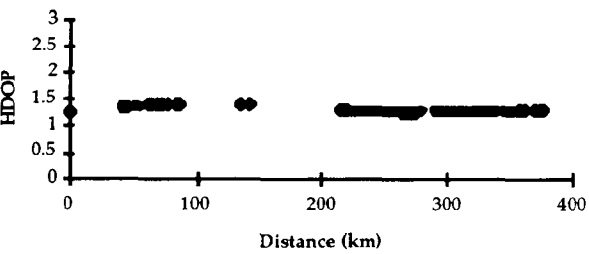
Québec to Havre-St-Pierre, TDs = 5930X
5930Y 5930Z



Québec to Carleton, TDs = 5930XYZ



Québec to Baie-Comeau, TDs = 5930X 5930Y 9960W
9960X



Québec to Ste-Anne-des-Monts, TDs = 5930X 5930Y
9960W 9960X

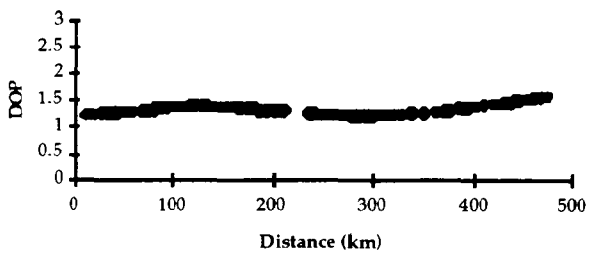
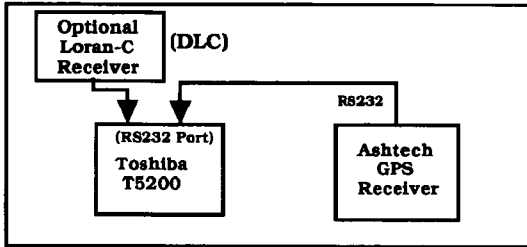


FIG. 3.- Loran-C HDOP Along the St. Lawrence River Using the Northeast U.S. Chain (9960), the Canadian East Coast Chain (5930) and a Combination of both Chains.

Monitor Set-up (On-Shore)



Remote Set-up (Vehicle/Ship)

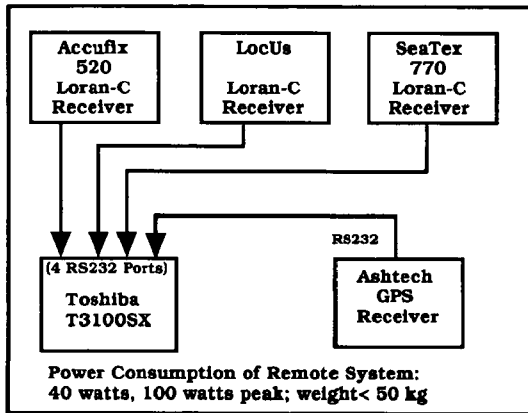


FIG. 4.- LORCAL² System Configuration.

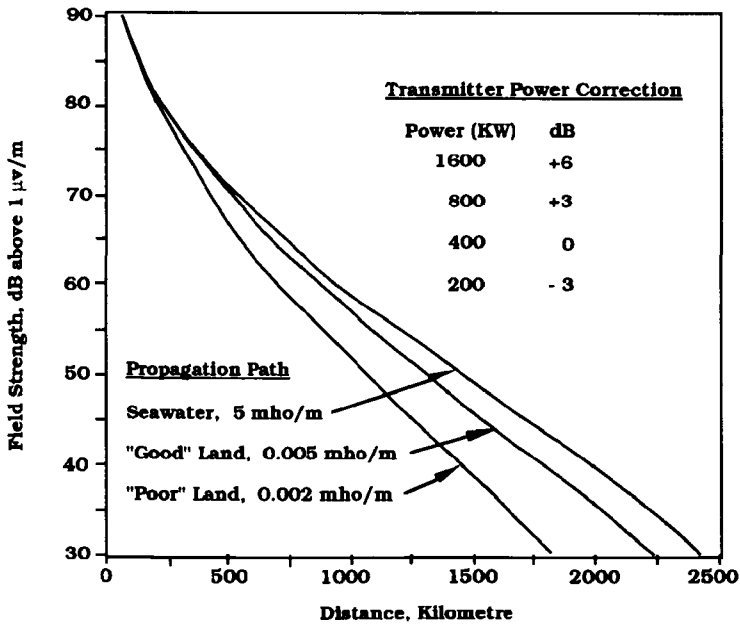


FIG. 5.- Field Strength at 100 kHz as a Function of Distance and Transmitted Power for Selected Ground Conductivities.

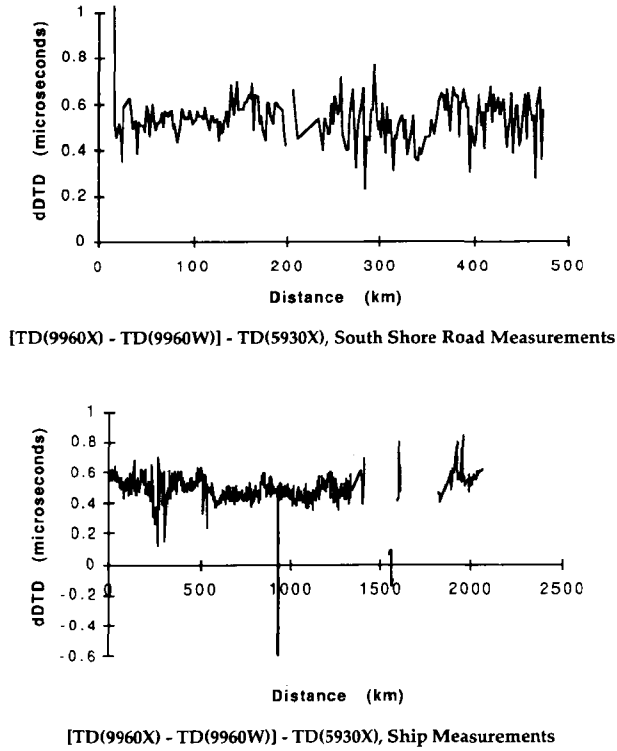


FIG. 6.- Across-Chain Loran-C Time Difference Comparison.

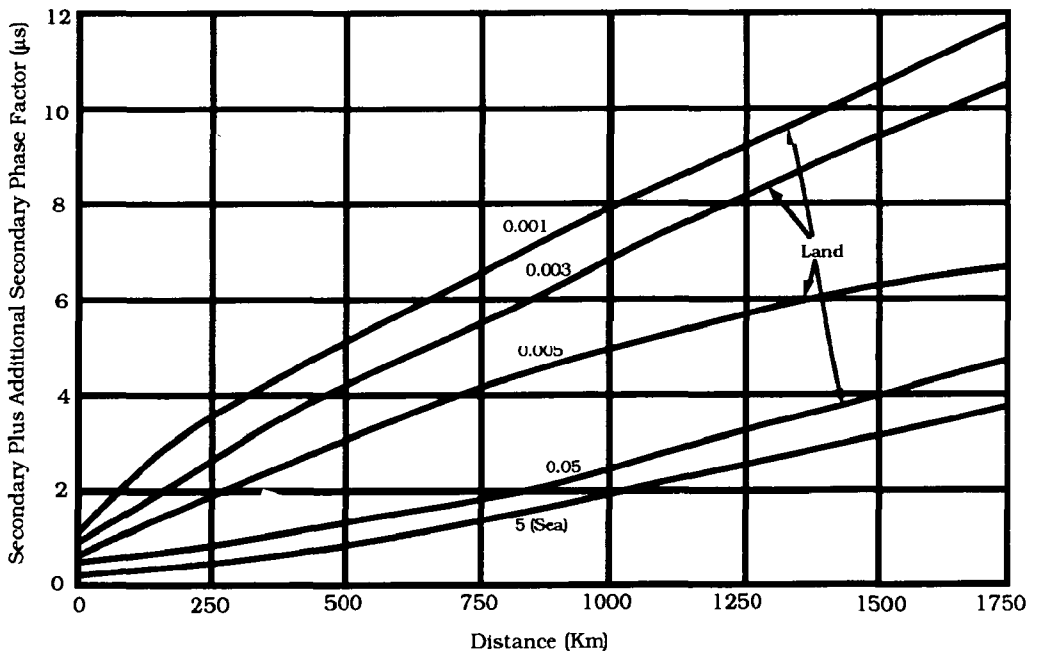
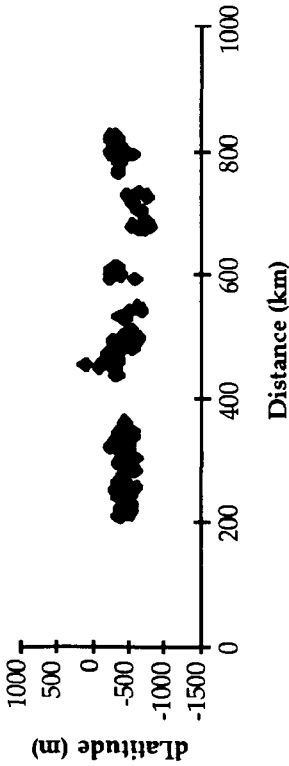
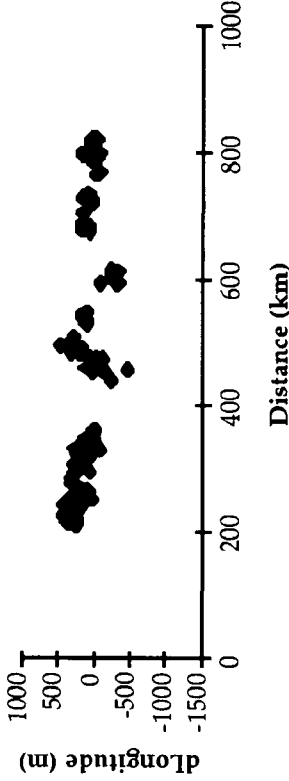


FIG. 7.- Combined Effect of Secondary (SF) and Additional Secondary Phase Lags (ASF) at 100 kHz as a Function of Distance for Selected Conductivities.

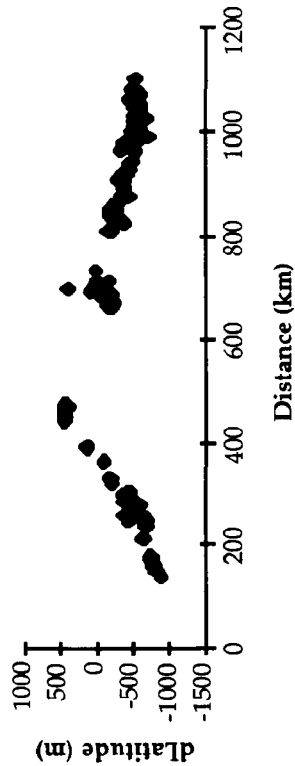
Québec to Havre-St-Pierre, PF = 320 ppm, Cnd = 5 S/m, TDs = 5930X 5930Y 5930Z, Mean = -434 m, RMS = 457 m, Std. Dev. = 141 m



Québec to Havre-St-Pierre, PF = 320 ppm, Cnd = 5 S/m, TDs = 5930X 5930Y 5930Z, Mean = 115 m, RMS = 208 m, Std. Dev. = 173 m



Québec to Carleton, PF = 320 ppm, Cnd = 5 S/m, TDs = 5930X 5930Y 5930Z, Mean = -371 m, RMS = 461 m, Std. Dev. = 274 m



Québec to Carleton, PF = 320 ppm, Cnd = 5 S/m, TDs = 5930X 5930Y 5930Z, Mean = 168 m, RMS = 318 m, Std. Dev. = 275 m

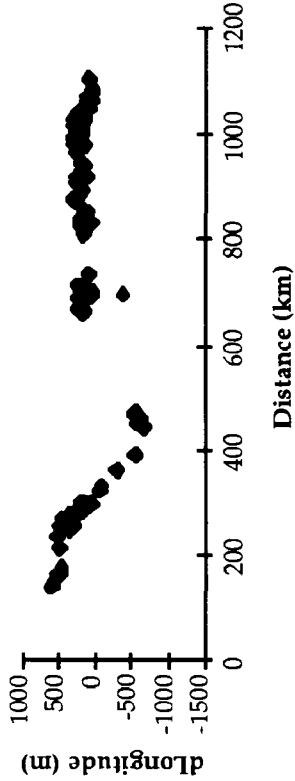
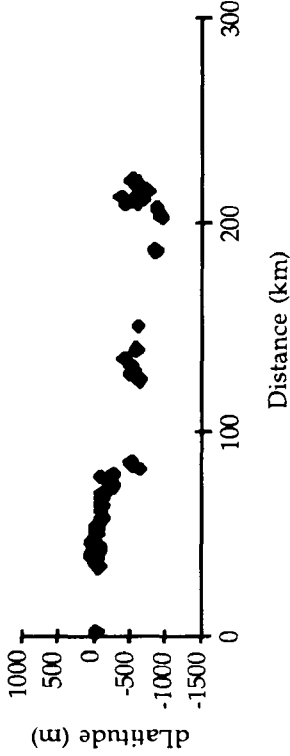
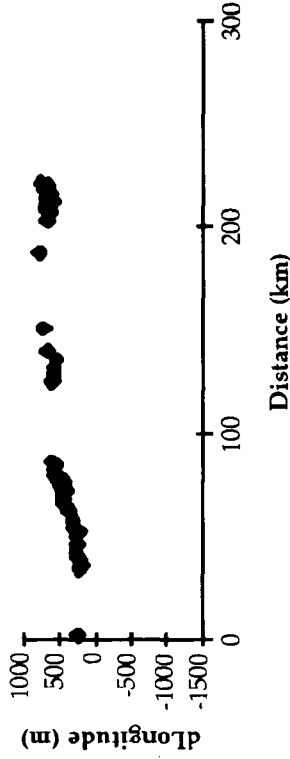


FIG. 8.- ASF Effect on Loran-C Positions Along the North and South Shores of the St. Lawrence Using 5930X, 5930Y, and 5930Z Transmitters.

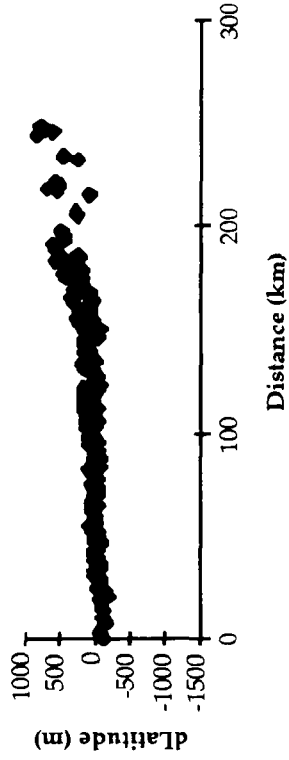
Québec to Tadoussac, PF = 320 ppm, Cnd = 5 S/m,
TDs = 9960W 9960X, Mean = -331 m, RMS = 443 m,
Std. Dev. = 295 m,



Québec to Tadoussac, PF = 320 ppm, Cnd = 5 S/m,
TDs = 9960WX, Mean = 489 m, RMS = 519 m, Std.
Dev. = 176 m



Québec to Rimouski, PF = 320 ppm, Cnd = 5 S/m,
TDs = 9960W 9960X, Mean = 165 m, RMS = 221 m,
Std. Dev. = 195 m



Québec to Rimouski, PF = 320 ppm, Cnd = 5 S/m,
TDs = 9960W 9960X, Mean = 250 m, RMS = 254 m,
Std. Dev. = 43 m

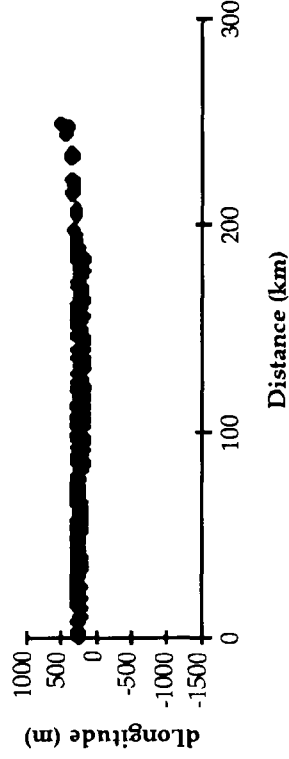
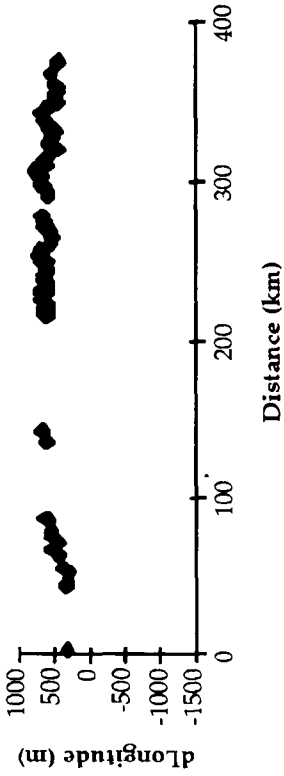
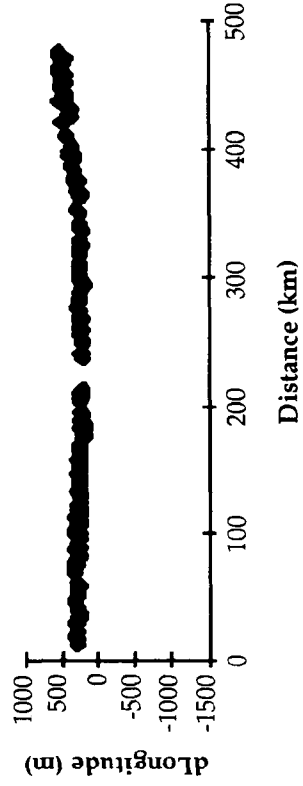


FIG. 9.-ASF Effect on LORAN-C Positions Along the North and South Shores of the St. Lawrence using 9960W and 9960X transmitters.

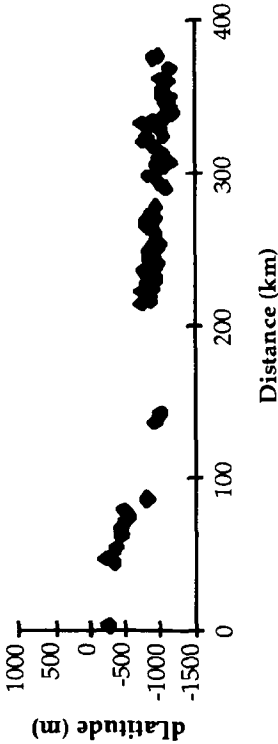
Québec to Baie-Comeau, PF = 320 ppm, Cnd = 5 S/m,
 TDs = 5930X 5930Y 9960W 9960X, Mean = 574 m,
 RMS = 582 m, Std. Dev. = 97 m



Québec to Ste-Anne-des-Monts, PF = 320 ppm, Cnd =
 5 S/m, TDs = 5930X 5930Y 9960W 9960X, Mean = 293
 m, RMS = 304 m, Std. Dev. = 84 m



Québec to Baie-Comeau, PF = 320 ppm, Cnd = 5 S/m,
 TDs = 5930X 5930Y 9960W 9960X, Mean = -863 m,
 RMS = 891 m, Std. Dev. = 221 m



Québec to Ste-Anne-des-Monts, PF = 320 ppm, Cnd =
 5 S/m, TDs = 5930X 5930Y 9960W 9960X, Mean = -606
 m, RMS = 699 m, Std. Dev. = 348 m

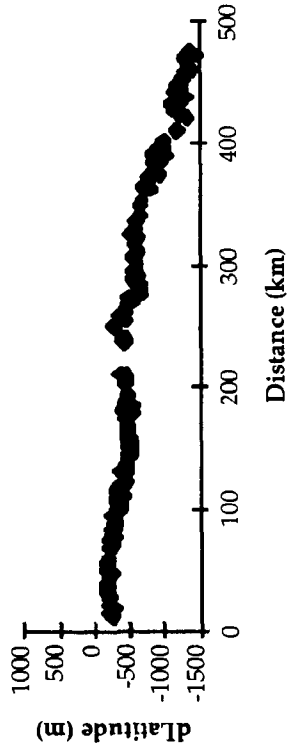
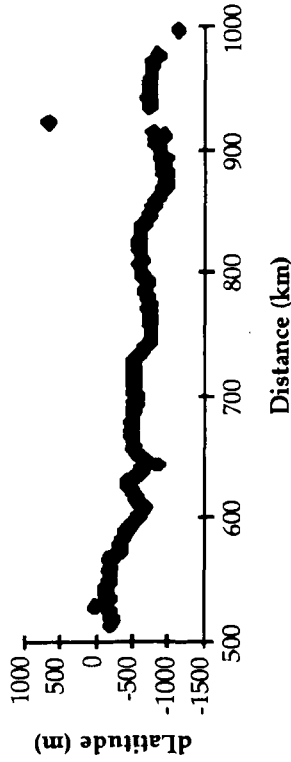


FIG. 10.- ASF Effect on Loran-C Positions Along the North and South Shores of the St. Lawrence Using 5930X, 5930Y, 9960W and 9960X Transmitters.

Ship, PF = 320 ppm, Cnd = 5 S/m, TDs = 5930X 5930Y
9960W 9960X, Mean = 589 m, RMS = 634 m, Std. Dev.
= 232 m



Ship, PF = 320 ppm, Cnd = 5 S/m, TDs = 5930X 5930Y
9960W 9960X, Mean = 325 m, RMS = 344 m, Std. Dev.
= 114 m

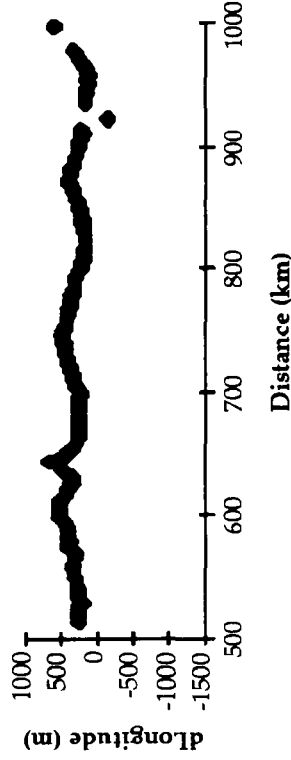


FIG. 11.- ASF Effect on Loran-C Positions in the St. Lawrence Between Québec City and Baie-Comeau Using 5930X, 5930Y, 5930Z, 9960W and 9960X Transmitters.

Table 1
Predicted Atmospheric Noise in the Lower St. Lawrence Area

Time Interval	Winter	Summer
0000 - 0400h	37.5 dB	49.5 dB
0400 - 0800	32.5	35.5
0800 - 1200	22.5	32.5
1200 - 1600	22.5	37.5
1600 - 2000	29.5	37.5
2000 - 2400	35.5	47.5

Predictions based on CCIR data (1988a).

Table 2
Predicted Versus Observed FS and SNR
(Winter 91 Observation Campaign)

Location	Latitude	Longitude	Date	Time	Actual			Pred. Meas.		Pred.		
					FS	FS	dFS	Noise	SNR	SNR	dSNR	dSNR _{Nc}
9960M												
Beauport	46 51 10	-71 12 3	March 19	06h	64	63	1	32	5	32	-27	2
Rivière-du-Loup	47 57 5	-69 27 52	March 19	21h	59	57	2	34	0	25	-25	3
Rimouski	48 35 6	-68 17 25	March 21	23h	56	53	3	36	-4	20	-24	2
Baie-Comeau	49 12 51	-68 11 41	March 20	08h	45	51	-7	27	0	18	-18	16
Sept-Iles	50 13 20	-66 23 15	March 20	17h	46	45	1	28	-10	17	-27	5
Gaspé	48 46 40	-64 27 17	March 17	11h	38	44	-6	23	-15	15	-31	8
9960W												
Beauport	46 51 10	-71 12 3	March 19	06h	77	83	-6	32	7	45	-38	-9
Rivière-du-Loup	47 57 5	-69 27 52	March 19	21h	82	88	-6	34	7	48	-41	-14
Rimouski	48 35 6	-68 17 25	March 21	23h	78	86	-8	36	7	42	-35	-10
Baie Comeau	49 12 51	-68 11 41	March 20	08h	72	82	-10	27	7	45	-38	-4
Sept-Iles	50 13 20	-66 23 15	March 20	17h	72	74	-2	28	7	44	-37	-4
Gaspé	48 46 40	-64 27 17	March 17	11h	66	77	-11	23	5	44	-39	0
9960X												
Beauport	46 51 10	-71 12 3	March 19	06h	60	61	-1	32	4	28	-24	5
Rivière-du-Loup	47 57 5	-69 27 52	March 19	21h	60	56	4	34	2	26	-24	3
Rimouski	48 35 6	-68 17 25	March 21	23h	53	53	0	36	-6	17	-23	2
Baie Comeau	49 12 51	-68 11 41	March 20	08h	47	51	-4	27	2	20	-18	16
Gaspé	48 46 40	-64 27 17	March 17	11h	50	49	1	23	-5	28	-33	6
5930M												
Beauport	46 51 10	-71 12 3	March 19	06h	78	83	-5	32	23	46	-23	6
Rivière-du-Loup	47 57 5	-69 27 52	March 19	21h	84	88	-4	34	19	51	-32	-5
Rimouski	48 35 6	-68 17 25	March 21	23h	86	86	0	36	20	50	-31	-6
Baie Comeau	49 12 51	-68 11 41	March 20	08h	78	82	-4	27	22	51	-29	5
Sept-Iles	50 13 20	-66 23 15	March 20	17h	76	74	2	28	16	47	-31	2
Gaspé	48 46 40	-64 27 17	March 17	11h	76	77	-1	23	19	53	-35	4
5930X												
Beauport	46 51 10	-71 12 3	March 19	06h	62	61	1	32	10	30	-20	9
Rivière-du-Loup	47 57 5	-69 27 52	March 19	21h	65	56	9	34	1	31	-30	-3
Rimouski	48 35 6	-68 17 25	March 21	23h	55	53	2	36	-7	19	-26	-1
Baie Comeau	49 12 51	-68 11 41	March 20	08h	53	51	2	27	0	26	-26	8
Sept-Iles	50 13 20	-66 23 15	March 20	17h	53	46	7	28	-6	25	-31	2
Gaspé	48 46 40	-64 27 17	March 17	11h	59	49	10	23	7	37	-30	9
5930Y												
Beauport	46 51 10	-71 12 3	March 19	06h	44	38	6	32	-7	12	-19	10
Rivière-du-Loup	47 57 5	-69 27 52	March 19	21h	54	43	11	34	-9	20	-29	-2
Rimouski	48 35 6	-68 17 25	March 21	23h	55	46	9	36	-7	19	-26	-1
Baie Comeau	49 12 51	-68 11 41	March 20	08h	50	46	4	27	-2	23	-25	9
Sept-Iles	50 13 20	-66 23 15	March 20	17h	53	49	4	28	-6	25	-31	2
Gaspé	48 46 40	-64 27 17	March 17	11h	62	56	6	23	6	40	-34	5
5930Z												
Beauport	46 51 10	-71 12 3	March 19	06h	44	41	3	32	-6	12	-18	11
Rivière-du-Loup	47 57 5	-69 27 52	March 19	21h	40	46	-6	34	-23	6	-29	-2
Rimouski	48 35 6	-68 17 25	March 21	23h	48	51	-3	36	-15	12	-27	-2
Baie Comeau	49 12 51	-68 11 41	March 20	08h	35	52	-17	27	-16	8	-24	10
Sept-Iles	50 13 20	-66 23 15	March 20	17h	43	58	-15	28	-16	15	-31	2
Gaspé	48 46 40	-64 27 17	March 17	11h	55	59	-4	23	-1	33	-34	5

All FS and SNR values in dB (referred to $1\mu\text{V m}^{-1}$)

Pred. SNR = Measured FS - Predicted atmospheric noise

dSNR_{Nc} is based on the use of a predicted constant atmospheric noise value of 61 dB (U.S. DoT 1992)

Table 3
Forward-Reverse DTDs

Data Set		5930X	5930Y	5930Z	9960W	9960X
North Shore Winter 91	Mean	0.06 μ s	0.04 μ s	0.03 μ s	0.02 μ s	0.05 μ s
	RMS	0.16	0.22	0.22	0.14	0.13
South Shore Winter 91	Mean	-0.05	-0.19	-0.06	0.00	-0.01
	RMS	0.17	0.24	0.22	0.14	0.14
North Shore Summer 91	Mean	-0.01	-0.10	-0.08	-0.03	0.01
	RMS	0.15	0.22	0.24	0.22	0.24
South Shore Summer 91	Mean	0.03	-0.02	-0.04	0.08	0.06
	RMS	0.14	0.16	0.17	0.16	0.17

Table 4
Winter-Summer DTDs

Data Set		5930X	5930Y	5930Z	9960W	9960X
North Shore	Mean	-0.17 μ s	-0.17 μ s	-0.20 μ s	0.10 μ s	-0.09 μ s
	RMS	0.20	0.24	0.30	0.22	0.14
South Shore	Mean	-0.19	-0.24	-0.22	0.01	-0.17
	RMS	0.21	0.27	0.28	0.14	0.21

Table 5
Modelled - GPS - Derived DTDs, Road Profiles

Data Set		Transmitters				
		5930X	5930Y	5930Z	9960W	9960X
North Shore	Mean	2.33 μ s	3.57 μ s	3.22 μ s	-4.59 μ s	-1.96 μ s
no PF, SF, ASF	RMS	2.35	3.74	3.32	4.68	2.05
North Shore	Mean	0.52	1.16	1.60	-2.78	-1.77
PF, $\sigma = 5 \text{ S m}^{-1}$	RMS	0.56	1.30	1.70	2.85	1.85
North Shore	Mean	-1.77	-1.71	-0.46	-0.20	-1.57
PF, $\sigma = 0.001 \text{ S m}^{-1}$	RMS	1.78	1.85	1.40	0.45	1.65
South Shore	Mean	1.90	3.03	2.55	-3.56	-1.02
no PF, SF, ASF	RMS	1.98	3.46	2.91	3.66	1.16
South Shore	Mean	0.21	0.56	0.89	-1.72	-0.75
PF, $\sigma = 5 \text{ S m}^{-1}$	RMS	0.53	1.23	1.29	1.79	0.89
South Shore	Mean	-2.17	-2.39	-1.37	0.99	-0.46
PF, $\sigma = 0.001 \text{ S m}^{-1}$	RMS	2.20	2.44	1.48	1.09	0.62
Ship	Mean	1.95	3.01	2.94	-4.23	-1.50
no PF, SF, ASF	RMS	2.05	3.38	3.36	4.34	1.78
Ship	Mean	0.24	0.80	1.28	-2.26	-1.19
PF, $\sigma = 5 \text{ S m}^{-1}$	RMS	0.67	1.12	1.52	2.37	1.45
Ship	Mean	-1.94	-1.80	-0.91	0.33	-0.89
PF, $\sigma = 0.001 \text{ S m}^{-1}$	RMS	1.99	1.99	1.31	0.78	1.16

Table 6
Modelled Versus GPS-Derived DTDs¹, Ships Profiles

Data Set		Transmitters				
		5930X	5930Y	5930Z	9960W	9960X
no PF applied	Mean	1.95	3.01	2.94	-4.23	-1.50
	RMS	2.05	3.38	3.36	4.34	1.78
no SF+ASF applied	St. dev.	0.63	1.52	1.64	0.96	0.96
N = 320	Mean	1.32	2.22	2.31	-3.52	-1.40
	RMS	1.46	2.54	2.68	3.62	1.67
no SF+ASF applied	St. dev.	0.61	1.25	1.34	0.87	0.91
N = 320	Mean	0.24	0.80	1.28	-2.26	-1.19
	RMS	0.67	1.12	1.52	2.37	1.45
$\sigma = 5 \text{ S m}^{-1}$	St. dev.	0.62	0.79	0.82	0.72	0.83
N = 320	Mean	-1.43	-1.16	-0.35	-0.35	-1.02
	RMS	1.51	1.32	0.74	0.77	1.27
$\sigma = 0.005 \text{ S m}^{-1}$	St. dev.	0.48	0.64	0.65	0.69	0.76
N = 320	Mean	-1.94	-1.80	-0.91	0.33	-0.89
	RMS	1.99	1.99	1.31	0.78	1.16
$\sigma = 0.001 \text{ S m}^{-1}$	St. dev.	0.42	0.85	0.94	0.70	0.75

¹ All means, rms and standard deviations are in μ s